ELSEVIER

Bioelectrochemistry 57 (2002) 33–38

Bioelectrochemistry

www.elsevier.com/locate/bioelechem

Highly sensitive sensors based on the immobilization of tyrosinase in chitosan

Gang Wang, Jing-Juan Xu, Li-Hua Ye, Jun-Jie Zhu, Hong-Yuan Chen*

Department of Chemistry, Laboratory of Mesoscopic Materials and Chemistry, Institute of Analytical Science, Nanjing University, Nanjing 210093, China

Received 19 July 2001; received in revised form 9 November 2001; accepted 14 November 2001

Abstract

A novel tyrosinase biosensor has been developed for a subpicomolar detection of phenols, which is based on the immobilization of tyrosinase in a positively charged chitosan film on a glassy carbon electrode. It was found that chitosan cross-linked with (3-aminooryloxypropyl) dimethoxymethylsilane is beneficial for the immobilization of tyrosinase. The large microscopic surface area and porous morphology of chitosan matrix lead to high enzyme loading, and the enzyme entrapped in this matrix can retain its bioactivity and the positively charged surface of chitosan can also display a good anti-interference ability to the substances with positive charge. Hence, the resulting sensor offers a high-sensitivity (150 nA·nM^{-1}) for the monitoring of phenols, and the detection limit is as low as 5.0×10^{-11} M. Its response time is less than 2 s reaching 95% of the steady-state value. It may retain 75% of the activity for at least 70 days.

Keywords: Tyrosinase; Chitosan; Biosensor; Phenol; AFM

1. Introduction

Phenols are present in the wastewaters of large number of industries including coal conversion, petroleum refining, resins and plastics, wood preservation, dyes, chemicals and textiles [1]. Calorimeter and ultraviolet spectrophotometric analyses are commonly used for the determination of phenols as standard methods [2,3]. However, these procedures usually require time-costing, complicated sample pretreatment, low sensitivity. The electroanalytical techniques applied for direct determination of these compounds suffer a number of these drawbacks due to the high overvoltage.

Tyrosinase, known as polyphenol oxidase that is widely distributed in bacteria, fruits, vegetables and seafood products can catalyze the oxidation of phenols with the aids of molecular oxygen as an oxidant. Tyrosinase contains two binuclear copper-containing active sites, which present at least two distinct binding sites, one of which has an affinity to aromatic compounds (substrate site) and the other an affinity for a metal binding agent (oxygen site). It catalyzes two distinct oxidation reactions as shown in Fig. 1. In cycle 1, tyrosinase accomplishes the oxidation of monophenols by oxygen as it passes through four enzyme states (E_{deoxy}, E_{oxy}, $E_{oxy\text{-}M}$ and $E_{met\text{-}D}$). In cycle 2, *o*-diphenols are oxidized as the enzyme passes through five enzyme states (E_{deoxy}, E_{oxy}, $E_{oxy\text{-}D}$, E_{met} and $E_{met\text{-}D}$). The two cycles lead to the formation of *o*-quinones, which spontaneously react with each other to form oligomers [4]. So most of the biosensors are based on the detection of electroreduction quinone products of enzyme reaction at low potential [5–8]. A more sensitive electrode response is obtained when *o*-quinone is reduced via a catalytically active redox polymer [9] or suitable redox mediators according to the simplified Fig. 1 [10].

To retain the enzyme's specific biological function, their immobilization on solid matrix is a key factor in preparing biosensors. That is, the structure and thickness of materials used to immobilize enzyme should not induce a severe decrease of enzyme functionality.

In this paper, we initiate a systematic exploration of a natural polymer, chitosan, as a structural material for designing functional layers on carbon electrode surfaces. Chitosan is an *N*-deacetylated derivative of chitin, a natural

* Corresponding author. Tel.: +86-25-359-2409; fax: +86-25-359-4862.
E-mail address: hychen@netra.nju.edu.cn (H.-Y. Chen).

1567-5394/02/$ - see front matter
PII: S1567-5394(01)00174-8

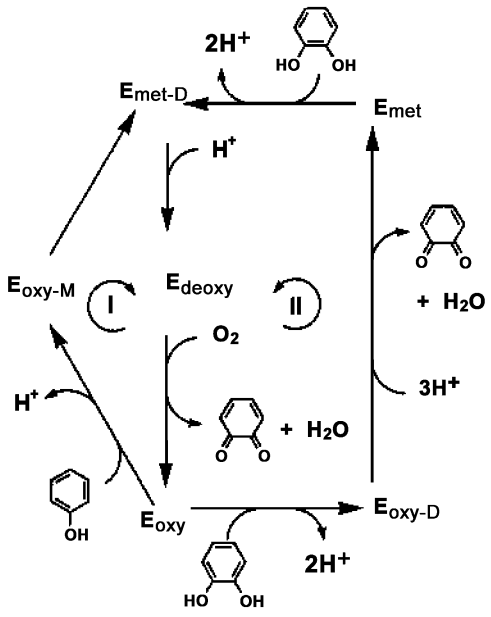

Fig. 1. Catalytic cycles for the: (1) hydroxylation of monophenols and (2) dehydrogenation of *o*-diphenols to *o*-quinones by tyrosinase. M = monophenol and D = diphenol.

occurring biopolymer found in the exoskeleton of crustaceans, in fungal cell wall, and in other biology materials [11]. Chitosan was selected here because of its unusual combination of property [12], which includes excellent membrane-forming ability, high permeability towards water, good adhesion, biocompatibility, nontoxicity, high mechanical strength and susceptibility to chemical modification due to the presence of reactive amino and hydroxyl functional group. Hexacyanoferrate (II) ($Fe(CN)_6^{4-}$) is chosen as an electron mediator because of its effective electron transferability [13]. Furthermore, this negatively charged mediator is expected to be firmly immobilized on the positively charged chitosan film through electrostatic interaction [14]. This design simplifies the fabrication procedure to obtain a highly sensitive (150 $nA \cdot nM^{-1}$) tyrosinase biosensor. The detection limit is 0.05 nM at signal-to-noise ratio of 3, the response time is less than 2 s reaching 95% of the steady-state value, and 75% of the activity is retained after 70 days.

2. Experimental

2.1. Reagents

Mushroom tyrosinase (from mushroom, EC 1.14.18.1), noted activity of ca. 4800 units/mg of solid (catalog T-7755), was purchase from Sigma (St. Louis, MO). Chitosan (MW $1.9–3.1 \times 10^5$; 92.5% deacetylation) was purchased from Nantong Shuanglin Co. Phenols, catechol, hydroquinone, *p*-nitrophenol and other chemicals were analytical grade and were used without further purification. Buffer solutions used in experiments were prepared with doubly distilled water.

2.2. Apparatus and measurements

Electrochemical measurements were done in a conventional three-electrode cell equipped with a platinum wire counter electrode, a saturated calomel reference electrode (SCE); all the potentials are reported vs. SCE, and a chitosan tyrosinase sensor as working electrode. Voltammetric measurements were carried out with the CHI660 electrochemical station (CH Instruments, USA). A magnetic stirrer provides the convective transport. All amperometric experiments were recorded at 25.0 ± 0.1 °C.

Fourier transform infrared (FT-IR) spectra by KBr pellets containing the chitosan films or chitosan/tyrosinase were obtained in the range of 4000–500 cm^{-1} on an Avatar 400 FT-IR spectrometer (Nicolet Instrument) at room temperature. The process of making films will be detailed below.

UV–visible absorption spectra were obtained with Shimazu UV-2400 spectrometer (Shimazu, Japan) at room temperature. The AFM experiments were carried out at room temperature using digital instrument nanoscope III (UAS) with a contact head and a 5 ~ μm scanner. Silicon nitrogen (Si_3N_4) cantilevers with nominal spring constant of 0.05 N m^{-1} and nominal resonance frequency in air of 22 kHz were used for contact mode in air; scan rates ranged 1–2 Hz in air.

2.3. Construction of tyrosinase biosensor

A 1.0-wt.% chitosan solution was prepared by dissolving chitosan flake in hot 0.05 $mol \cdot l^{-1}$ acetic acid (HAc). The solution was cooled to room temperature and filtered using a 0.45-μm syringe filter unit. This chitosan solution was cross-linked with 0.3-g (3-aoryloxypropyl) dimethoxymethylsilane for about 20 h.

A glassy carbon electrode (GCE, 3-mm diameter, Jiangsu Electroanalytical Instruments Factory, Jiangsu, China) was used as the base electrode for the preparation of the chitosan/tyrosinase biosensor. The GCE was polished with 1700 diamond paper, followed by 0.3, 0.2 μm alumina particles on chamois leather, rinsed thoroughly with doubly distilled water between each polishing step, then washed successively with 1:1 nitric acid, alcohol and doubly distilled water in an ultrasonic bath, and dried in air before use.

The surface of the electrode was first coated with chitosan-$Fe(CN)_6^{4-}$ by pipetting 10 μl of stock standard CHIT solution containing 50 mM $Fe(CN)_6^{4-}$. After drying under ambient temperature for 1 h, a thin film of CHIT–$Fe(CN)_6^{4-}$ was formed at the electrode surface. The immobilization of tyrosinase in the CHIT matrix was accomplished by the addition of 10 μl of 0.1 mg/ml tyrosinase to 10 μl of stock standard CHIT solution. With a micropipette, aliquots (10 μl) of such a colloid were deposited on the top

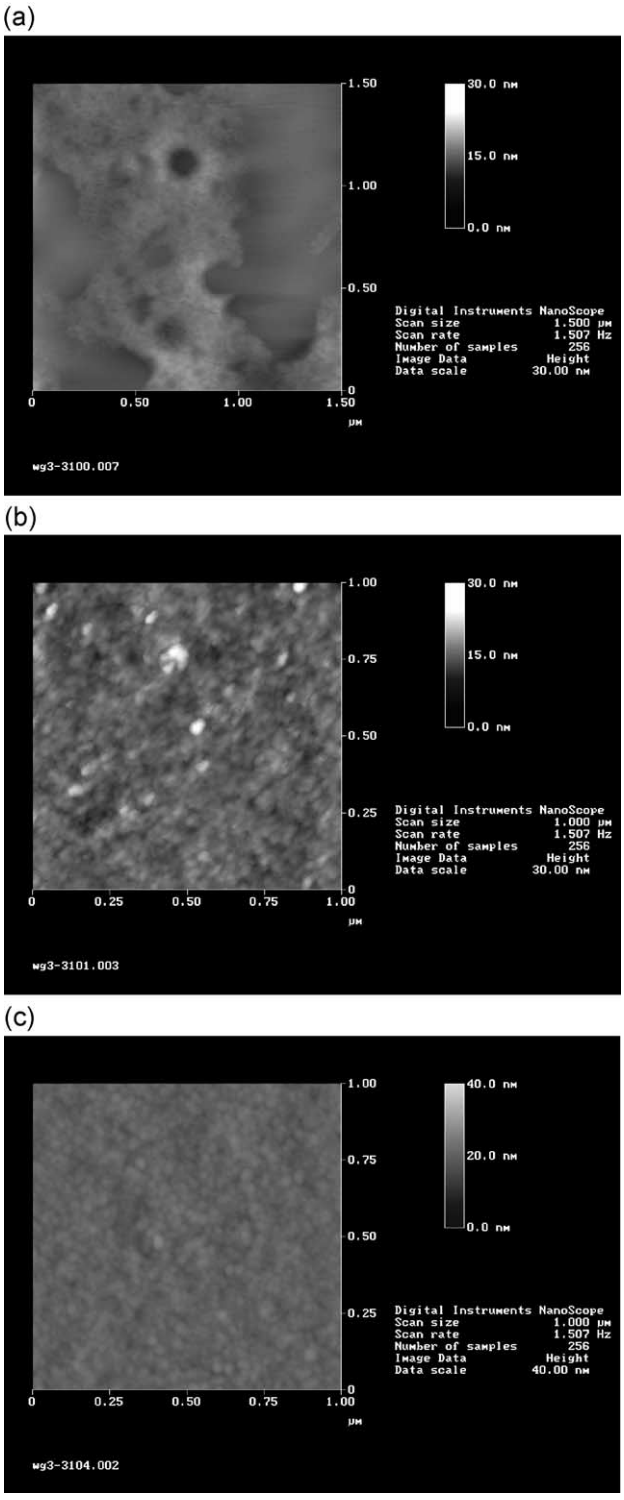

Fig. 2. Atomic force micrography of the thin films of (a) CHIT; (b) CHIT doped with $Fe(CN)_6^{4-}$; (c) CHIT doped with $Fe(CN)_6^{4-}$ and tyrosinase.

of the CHIT–$Fe(CN)_6^{4-}$ surface and allowed to dry for 1 day under ambient conditions for the solidification. The enzyme electrodes were thoroughly rinsed with doubly distilled water and equilibrated in stirred pH 7.4 phosphate buffer solution for at least 2 min to allow the background current to diminish to a steady value. When not in use, the enzyme electrodes were stored in air at 4 °C.

3. Results and discussion

3.1. Morphologies of CHIT, CHIT–$Fe(CN)_6^{4-}$ and CHIT–$Fe(CN)_6^{4-}$–tyrosinase films

The physical morphology of the CHIT matrix may effect on the performance of the enzyme electrode. The morphologies of CHIT, CHIT–$Fe(CN)_6^{4-}$, and CHIT–$Fe(CN)_6^{4-}$–tyrosinase films were characterized by atomic force microscopy (AFM). A typical AFM picture of the CHIT membrane displays a three-dimensional porous network (Fig. 2a). This uniform porous structure provided a significantly enhanced enzyme loading of the enzyme electrodes. When $Fe(CN)_6^{4-}$ was immobilized in the CHIT matrix, many smaller particles appeared, which were $Fe(CN)_6^{4-}$ domains (Fig. 2b). The aggregation of the intercalative molecules distributes regularly and has island structures. When tyrosinase was entrapped on the CHIT–$Fe(CN)_6^{4-}$ film, more denser dot-shaped particles were distributed uniformly on the surface (Fig. 2c).

3.2. Intermolecular interaction between CHIT and $Fe(CN)_6^{4-}$

Due to the positive charge of the CHIT and the strong adsorptive properties, it would strongly interact with the negatively charged $Fe(CN)_6^{4-}$ by electrostatic interaction

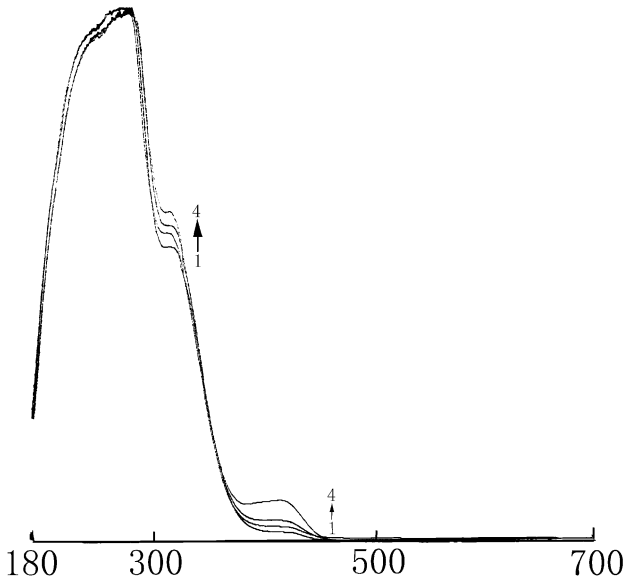

Fig. 3. UV–visible absorption spectra of $Fe(CN)_6^{4-}$ dissolved in (1) water; (2) in CHIT (24 h); (3) in CHIT 48 h; and (4) in CHIT 96 h.

resulting in the immobilization of $Fe(CN)_6^{4-}$. The interactions between CHIT and $Fe(CN)_6^{4-}$ were investigated by employing UV–visible absorption spectra. Fig. 3 shows the difference between the visible absorption spectrum of $Fe(CN)_6^{4-}$ dissolved in water and dissolved in CHIT solution. The adsorption band of $Fe(CN)_6^{4-}$ dissolved in water was observed at 450 nm, and the strength did not change during storage. When the $Fe(CN)_6^{4-}$ dissolved in CHIT solution, its absorption band shifted to 410 nm and the intensity became stronger with the increasing storage time. The results showed that $Fe(CN)_6^{4-}$ was interacted with CHIT and it could be incorporated in the CHIT films and made it more stable.

3.3. Intermolecular interaction between CHIT and tyrosinase

The interactions between CHIT and tyrosinase were studied by infrared spectra and UV–visible spectra. The Fourier transform infrared spectra of CHIT (1) and tyrosinase/CHIT (2) are shown in Fig. 4a. The adsorption band at 1075 cm^{-1} of CHIT is the characteristics of frame symmetric and asymmetric flexible vibrations. When tyrosinase was immobilized on the CHIT, there were some differences between the IR spectra of CHIT and tyrosinase/CHIT. The adsorption band at 1197 cm^{-1} disappeared and the band at 1618 cm^{-1} shifted to 1659 cm^{-1} in the IR adsorption of

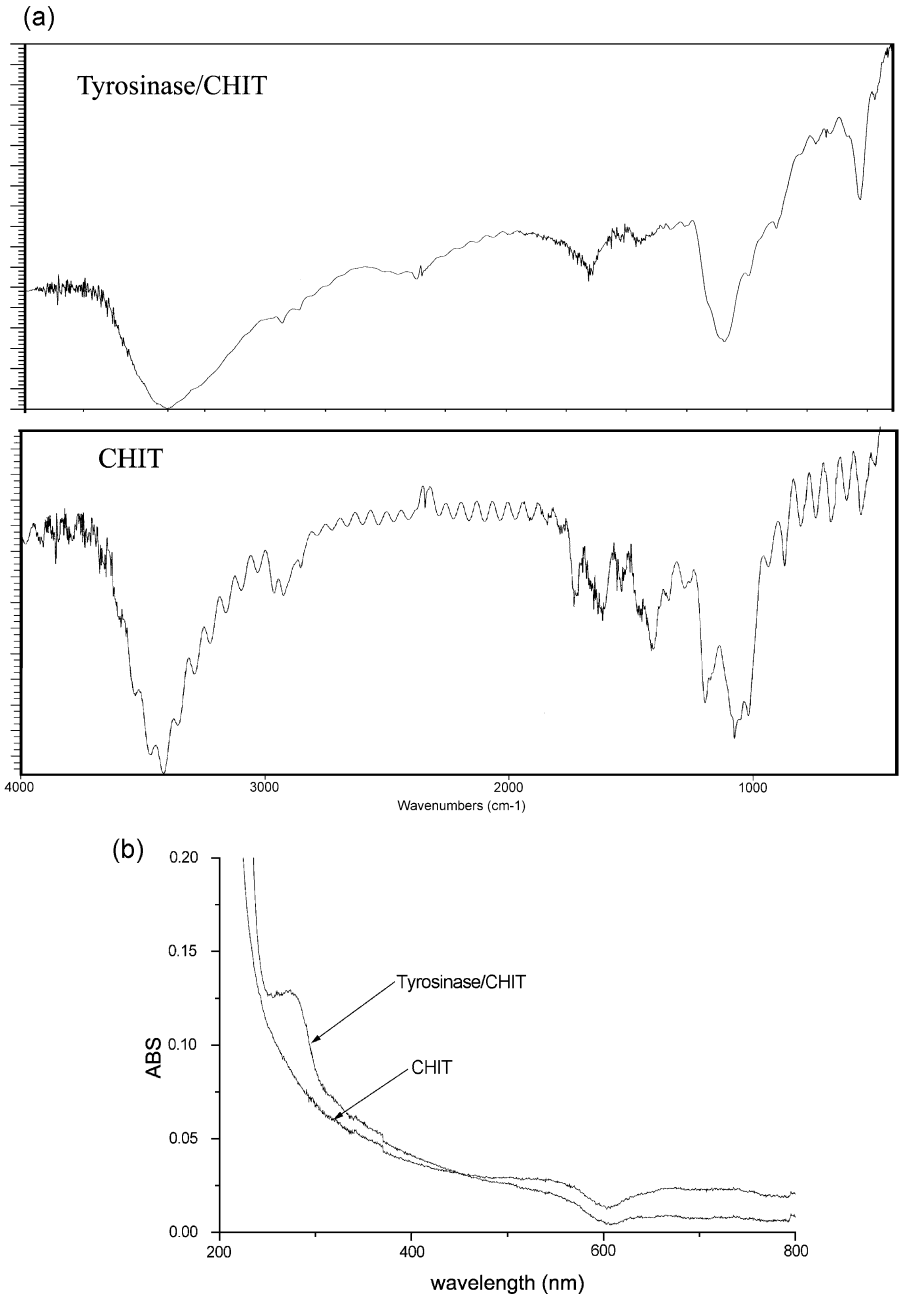

Fig. 4. FT-IR (a) and UV–visible (b) spectra of CHIT and tyrosinase/CHIT.

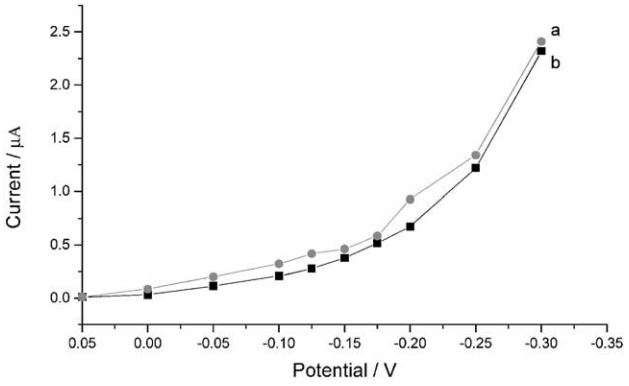

Fig. 5. Effect of working potential on the response current of the enzyme electrode in air-saturated 0.025 M phosphate buffer solution (pH 7.4) with stirring at 25.0 ± 0.1 °C with (a) and without (b) 1.0×10^{-6} M phenol solution.

tyrosinase/CHIT. There were also changes in both the NH stretching and NH bending regions of IR spectra. In the NH stretching region (3200–3500 cm^{-1}), primary amines have two typical bands while secondary amines have a single band. And there was a small decrease in 3414 cm^{-1} after the interaction which was consistent with the conversion of some primary amino groups of chitosan. These results showed that there were the molecular interactions between tyrosinase and some specific site of the CHIT and apparently the CHIT was a good immobilization matrix for enzymes. Fig. 4b showed that the UV–visible absorbance of the film was increased substantially when a CHIT film reacted with tyrosinase. The broad peak at 275 nm for the "reacted CHIT film" suggested that the tyrosinase was covalently grafted to the CHIT film [15].

3.4. Amperometric response of tyrosinase biosensor

3.4.1. The dependence of the current response of tyrosinase biosensor on working potential and pH

The various experimental parameters, which can affect the amperometric determination of phenol, are optimized.

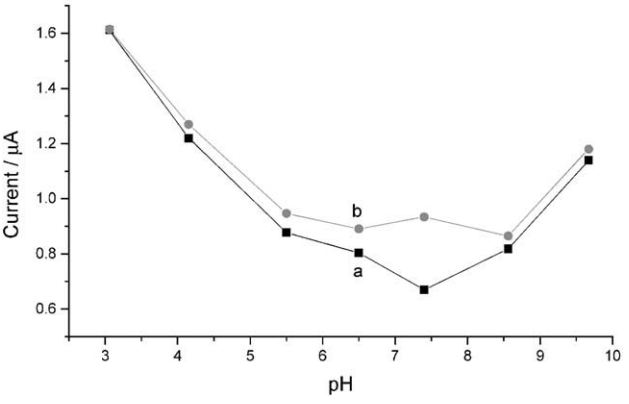

Fig. 6. Effect of pH of the buffer solution on the response of tyrosinase biosensor to 1.0×10^{-6} M phenol in 0.025 M phosphate buffer. Working potential − 0.20 V (vs. SCE), temperature 25.0 ± 0.1 °C.

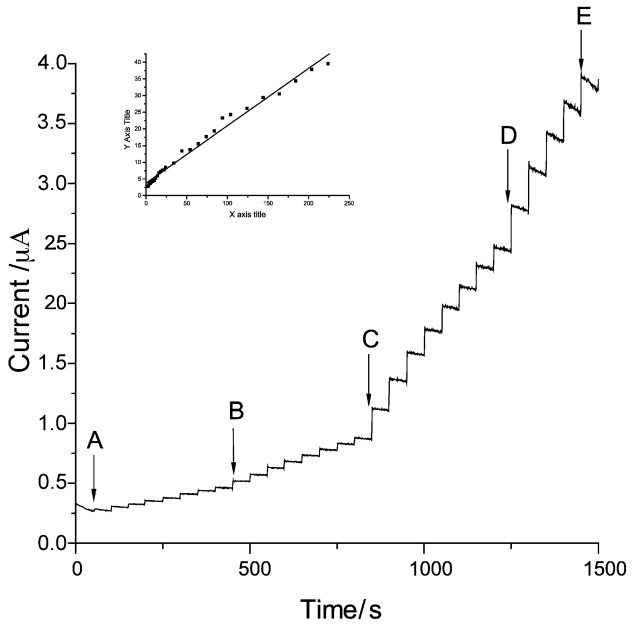

Fig. 7. Hydrodynamic response of the tyrosinase biosensor for phenol in air-saturated PBS upon the following concentration: A → B, in 1×10^{-10} M steps; B → C, in 2×10^{-10} M steps; C → D, in 1×10^{-9} M steps; D → E, in 2×10^{-9} M steps. Inset: the calibration curve of phenol.

The effect of applied potential on the amperometric signal and background current of the sensor was tested in the range between 0.10 and − 0.30 V. As can be seen in Fig. 5, an optimum ratio of signal-to-background current was obtained at − 0.20 V. Using working potentials negative than − 0.20 V, a higher signal current is obtained, but the background current also increases distinctly. Therefore, the working potential of − 0.20 V was selected for further studies. The effect of pH was also studied at different pH values in 0.025 M phosphate buffer (Fig. 6) at working potential − 0.20 V. Both currents of phenol and background decreased as the pH changed from 3.0 to 6.5, and the current of phenol increased from pH 6.4 to 7.4 while the current of background still decreased. This is accordance with the Ref. [9] and indicates that immobilization of enzyme does not drastically alter its pH response characteristics. The largest current difference between phenol and background was found

Table 1
Relative activity of the sensor for various phenolic compounds

Compound	Relative electrochemical activity (%)	Compound	Relative electrochemical activity (%)
Phenol	100	*p*-nitrophenol	0.0
Catechol	184.5	Dopamine	130.5
Hydroquinone	2.4	phloroglucin	19.9

The concentration of the detected compound was 1 μM. working potential − 0.20 V (vs. S.C.E.). The current response of the enzyme electrode to phenol is taken as 100%.

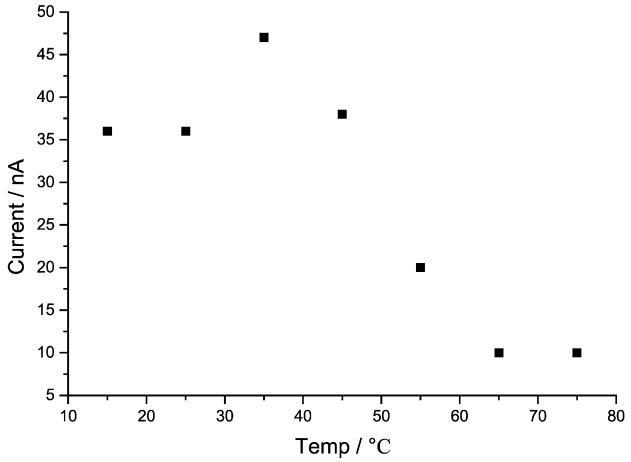

Fig. 8. Thermal stability of the tyrosinase biosensor.

at pH 7.4. Therefore, pH 7.4 was chosen for all subsequent studies.

3.4.2. Hydrodynamic response of phenol at the tyrosinase biosensor

Fig. 7 displays a typical current–time response using the enzyme electrode under the optimal experimental conditions after the addition of successive aliquots of phenol to the phosphate buffer solution under stirring. A well-defined reduction current proportional to the phenol concentration has been observed. The response to phenol is linear ($r = 0.9993$) in the range from 1.0×10^{-10} to 2.3×10^{-8} M. The limit of detection is 5.0×10^{-11} M (corresponding to 5.0×10^{-13} mol) at a signal-to-noise ratio of 3. The reproducibility of the response of the enzyme electrode was investigated at a phenol concentration of 1.5×10^{-8} M; the mean current was 0.638 μA with a relative standard deviation of 1.9%. For a series of 10 sensors prepared according to the same procedure, a relative standard deviation of 4.9% was obtained for the same phenol solution. These good results may be attributed to the uniform structure of CHIT matrix formed. The responses for phenol-derivative compounds obtained at -0.20 V were also investigated; the same results have been obtained of catechol, hydroquinone, and *p*-nitrophenol (shown in Table 1).

3.5. Interference studies

When the concentration of phenol was 1 μM, the interference effects were investigated by testing the response of the enzyme electrode to 50 times of cysteine, 2500 times of glucose, 2500 times of acetaminophenol, 500 times of uric acid, 500 times of ascorbic acid and 5000 times of hydrogen peroxide. It was found that these substances did not cause any observable interference in the determination of phenol except ascorbic acid and hydrogen peroxide because ascorbic acid could reduce *o*-qiunone and hydrogen peroxide could oxidize phenol.

3.6. Thermal and storage stability of the tyrosinase biosensor

The current response of this biosensor was measured in the temperature range 15–75 °C (Fig. 8). The response gradually increased and reached a maximum level at 35 °C and then fell sharply when the temperature was higher than 45 °C, which indicated that the enzyme was denatured.

The sensors' storage stability was examined by storing it in a pH 7.4 PBS at 4 °C over 2 months, with intermittently measuring the current response to phenol standard solution every 2–3 days. The results showed that the activity of the sensor reached a maximum after a few days, and then reduced gradually. The catalytic current response could maintain about 75% after storage for 70 days.

Acknowledgements

The financial support by the National Natural Science Foundation of China (grant no. 29835110, 20075010) is gratefully acknowledged.

References

[1] J. Karam, J.A. Nicell, Potential applications of enzyme in waste treatment, J. Chem. Technol. Biotechnol. 69 (1997) 141–153.
[2] A. Townshend (Ed.), Encyclopedia of Analytical Science, vol. 8, Academic Press, London, 1995, p. 3298.
[3] A.I. Vogel, Textbook of Quantitative Chemical Analysis, Longman, Essex, UK, 1998, p. 707.
[4] J. Dec, J.-M. Bollag, Effect of various factors on dehalogenation of chlorinated phenols and anilines during oxidative coupling, Environ. Sci. Technol. 29 (1995) 657–663.
[5] M.H. Smit, G.A. Rechnitz, Toxin detection using a tyrosinase-coupled oxygen electrode, Anal. Chem. 65 (1993) 380–385.
[6] P. Oennerfjord, J. Emneus, G. Marko-Varga, L. Gorton, Tyrosinase graphite-epoxy based composite electrode for detection of phenols, Biosens. Bioeletron. 10 (1995) 607–619.
[7] E.S.M. Lutz, E. Dominguez, Development and optimization of a solid composite tyrosinase biosensor for phenol detection in flow injection systems, Electroanalysis 8 (1996) 117–123.
[8] E. Burestedt, A. Narvaez, T. Ruzgas, L. Gorton, J. Emneus, E. Dominguez, G. Marko-Varga, Rate limiting steps of tyrosinase-modified electrode for detection of catechol, Anal. Chem. 68 (1996) 1605–1611.
[9] F. Daigle, D. Leech, Reagentless tyrosinase enzyme electrode: effects of enzyme loading, electrolyte pH, ionic strength and temperature, Anal. Chem. 69 (1997) 4108–4112.
[10] H. Kotte, B. Grundig, K.D. Vorlop, B. Strehlitz, U. Stottmeister, Methylphenazonium-modified and enzyme sensor based on polymer thick films for subnanomolar detection of phenols, Anal. Chem. 67 (1995) 65–70.
[11] M.G. Peter, Applications and environment aspects of chitin and chitosan, J. Macromol. Sci., Pure Appl. Chem. A 32 (1995) 629–640.
[12] R.A.A. Muzzarelli, Chitin, Pergamon, Oxford, 1977, p. 140.
[13] J.G. Schiller, A.K. Chen, C.C. Liu, Determination of phenol concentrations by a electrochemical system with immobilized tyrosinase, Anal. Biochem. 85 (1978) 25–33.
[14] X. Qu, A. Wirsen, A.-C. Albertsson, Novel pH-sensitive chitosan hydrogels: swelling behavior and states of water, Polymer 41 (2000) 4589–4598.
[15] G. Kumar, J.F. Briston, P.J. Smith, G.F. Payne, Enzyme gelation of natural polymer chitosan, Polymer 41 (2000) 2157–2168.